Novel porcine model of implant-associated osteomyelitis

A comprehensive analysis of local, regional, and systemic response

Jensen, Louise Kruse; Koch, Janne; Dich-Jørgensen, Kristine; Aalbaek, Bent; Petersen, Andreas; Fuursted, Kurt; Bjarnsholt, Thomas; Kragh, Kasper Nørskov; Tøtterup, Mikkel; Bue, Mats; Hanberg, Pelle; Søballe, Kjeld; Heegaard, Peter M H; Jensen, Henrik Elvang

Published in:
Journal of Orthopaedic Research

DOI:
10.1002/jor.23505

Publication date:
2017

Document version
Peer reviewed version

Research Article

A novel porcine model of implant associated osteomyelitis: a comprehensive analysis of local, regional and systemic response[†]

Running title: Porcine model of osteomyelitis

Louise Kruse Jensen[1], Janne Koch[2], Kirstine Dich-Jorgensen[1], Bent Aalbæk[1], Andreas Petersen[3], Kurt Fuursted,[3] Thomas Bjarnsholt[4,5], Kasper Nørskov Kragh[4], Mikkel Tøtterup[6,7], Mats Bue[6,8], Pelle Hanberg[6], Kjeld Søballe[6], Peter MH. Heegaard[9], Henrik Elvang Jensen[1].

[1]Department of Veterinary Disease Biology, Ridebanevej 3, 1870 Frederiksberg C, University of Copenhagen, Denmark

[2]Leo Pharma A/S, Industriparken 55, 2750 Ballerup, Denmark

[3]Statens Serum Institut, Artillerivej 5, 2300 Copenhagen S, Denmark

[4]Costerton Biofilm Center, Institute of Immunology and Microbiology, Blegdamsvej 3B, 2200 Copenhagen N, University of Copenhagen, Denmark

[5]Department of Clinical Microbiology, Juliane Maries Vej 22, 2100 Copenhagen Ø, Copenhagen University Hospital, Denmark

[6]Orthopedic Research Unit, Building 1A, Nørrebrogade 44, 8000 Aarhus, Aarhus University Hospital, Denmark

[7]Department of Orthopedic Surgery, Skovlyvej 15, 8930 Randers NØ, Randers Regional Hospital, Denmark

[8]Department of Orthopedic Surgery, Sundvej 30, 8700 Horsens, Horsens Regional Hospital, Denmark

[9]Innate Immunology Group, National Veterinary Institute, Bülowsvej 27, 1870 Frederiksberg C, Technical University of Denmark, Denmark

Corresponding author:
Louise Kruse Jensen, Department of Veterinary Disease Biology, Ridebanevej 3, 1870 Frederiksberg C, University of Copenhagen, Denmark
Tlf: 22165332
Email: louise-k@sund.ku.dk

[†]This article has been accepted for publication and undergone full peer review but has not been through the copyediting, typesetting, pagination and proofreading process, which may lead to differences between this version and the Version of Record. Please cite this article as doi: [10.1002/jor.23505]

Received 28 September 2016; Revised 21 November 2016; Accepted 5 December 2016

Journal of Orthopaedic Research

DOI 10.1002/jor.23505

Author Contributions Statement: LKJ, JK, MT, MB, KS and HEJ designed the study. LKJ, JK, KDJ, MT, PH, and MB performed the surgical insertion of bone implants. LK and KDJ performed the necropsies. PMHH analyzed blood samples for acute phase proteins. BA, TB, KKN, KF and AP performed the microbiology *e.g*. inoculum, screening for bacteremia, swab analysis, PNA FISH of implants and *spa*-typning. LKJ and HEJ performed histopathology. LKJ performed CT analysis, statistic calculations and drafted the manuscript. All authors read, revised and approved the final submitted manuscript.

Abstract

Pigs are favorable experimental animals for infectious diseases in humans. However, implant associated osteomyelitis (IAO) models in pigs have only been evaluated using high-inoculum infection (>10^8 CFU) models in 1975 and 1993. Therefore, the aim of this paper was to present a new low inoculum porcine model of human IAO based on 42 experimental pigs. The model was created by drilling an implant cavity in the tibial bone followed by insertion of a small steel implant and simultaneous inoculation of *Staphylococcus aureus* bacteria (n=32) or saline (n=10). The infected pigs were either inoculated with 10^4 CFU (n=26) or 10^2 and 10^3 CFU (n=6). All animals were euthanized five days after insertion of implants. Pigs receiving the high-inoculum infections showed a significantly higher volume of bone lesion, number of neutrophils around the implant, concentrations of acute phase proteins in serum and enlargement of regional lymph nodes. A positive correlation was present between a high number of surrounding neutrophils and high values of all other parameters. Furthermore, a threshold of 40 neutrophils per 10 high power fields for the histopathological diagnosis of high grade IAO was defined. In conclusion: this paper describes a novel low-inoculum *S. aureus* porcine model of IAO which was demonstrated to be reliable, reproducible and discriminative to human IAO, and represents a requested and valuable tool in orthopedic research.

Key words: Animal model, Osteomyelitis, Peri-prosthetic Infection, *S. aureus*

Introduction

Orthopedic implants have become an essential component of modern medicine (1). The number of operations with insertion of orthopedic implants is increasing, *e.g.* in the UK and USA 800 000 joint arthroplasties are completed annually, with projections of up to 4 million by 2030 (1). However, up to 5 percent of patients with an orthopedic implant will develop osteomyelitis around the implant (2, 3). Implant associated osteomyelitis (IAO) or prosthetic joint infections is among the most severe orthopedic conditions and treatment failure is common (4, 5). In order to reduce the incidence of treatment failure and increase the success of prevention and diagnosis, more research on IAO is needed. In experimental studies of IAO it is crucial to study the surface of the implant, the local bone tissue surrounding the implant and the systemic reactions simultaneously. However, this can only be achieved in a reliable, reproducible and discriminative animal model of IAO. Pigs have drawn growing attention as experimental animals in recent years, and should be advantageous in infective orthopedic research due their comparable immune system, bone anatomy and pathophysiology (6). However, pigs have only been used twice in 1975 (7) and 1993 (8) as models for IAO. Therefore, in the present study we aimed to describe a novel porcine IAO model in detail, *i.e.* surgical implantation technique and quantification of the systemic, regional and local outcome.

Material and methods

Design

The model was based on insertion of a small steel implant into the right tibial bone together with either bacteria or saline. Based on inoculum, pigs were allocated into 3 groups, *e.g.* high-inoculum dose (10^4 CFU; Group A), low-inoculum dose (10^2 or 10^3 CFU; Group B) and controls

(Saline; Group C), (Table 1). The Danish Animal Experiments Inspectorate approved the experimental protocol (license No. 2013/15-2934-00946).

Animals

A total of 42 female Danish Landrace pigs obtained from specific pathogen free herds (9) were included. The age of the pigs were either 3 months (30-kilogram body weight (BW)) or 8 months (67-77-kilogram BW), (see Table 1). Ten pigs from Group A (Table 1) were basis for a study of antibiotic penetration into inflamed bone tissue, and data from this study, pathology excluded, was recently published elsewhere (10). At arrival the animals were allowed to acclimatize for 7 days before entering the trial.

Anesthetic, analgesic, antibiotic and euthanization protocol

Premedication, induction of anesthesia and intraoperative analgesic were induced as described recently (11). Anesthesia was maintained with Propofol (10 mg/kg BW/hour) and intraoperative analgesia with Fentanyl (0.5 mg/hour). At the end of surgery, animals received an intramuscular injection 0.1 mg/kg BW of Buprenorphine (0.3mg/ml) resulting in postoperative analgesia for the following 6 hours. Thereafter the animals received oral analgesic treatment with Meloxicam 0.3 mg/kg BW once a day. After skin closure antibiotic ointment was applied to the surgical wound (Fucidin, LEO Farma, Ballerup, Denmark) to prevent infections from the environment (11). No systemic antibiotic treatment was given. All pigs were euthanized after 5 days by an intravenous overdose of pentobarbital 20 %.

Surgical procedure

Pigs were placed in right lateral recumbency exposing the medial side of the right tibial bone. On

the medial side the tibial tuberosity and crest is covered by the crucial fascia, subcutis and skin. This non-muscular area, positioned adjacent to trabecular bone tissue, was found ideal for insertion of the implant. The surgical procedure was performed under sterile conditions (Fig. 1A). Crista tibiae was located by palpation and a scalpel placed over the highest point of crista tibiae. A radiographic picture was obtained using mobile C-arm fluoroscopy. The position of the scalpel was adjusted until the final position for the implant cavity was achieved (located centrally and 10 mm distal and parallel to the growth plate). A skin incision of 20 mm was made over the final position followed by a second incision in the subcutaneous tissue down to the periosteum. The final incision of 10 mm was made in the periosteum, which was loosened a few mm perpendicular to the incision. In the periosteal incision a K-wire (4 mm in diameter) was drilled 20 mm (pigs of 30 kg BW) or 27 mm (pigs of 67-77 Kg BW) into the trabecular bone tissue creating the implant cavity. By placing a sterile cotton gaze pad in the implant cavity compression haemeostasis was achieved after 5 minutes. Afterwards the inoculum (10 μL) was injected (Figs. 1B + 1C). Injection of inoculum was performed using a pipette with a sterile changeable tip. The tip was placed in the bottom of the drill hole during the injection. Thereafter, the implant was inserted into the cavity. Implants were made of stainless steel, 2 x 15 mm (pigs of 30 kg BW) or 2 x 20 mm (pigs of 80 Kg BW). The periosteum, subcutaneous tissue and skin were sutured separately (Fig. 1D).

Postoperative care

Animals were followed up daily during the postoperative period and included surgical wound inspection, evaluation of gait and if indicated measurements of body temperature. Impaired ability to stand, anorexia and systemic signs of sepsis, *e.g.* depressed respiration and high fever, were set as humane endpoints.

Inoculum

A porcine *Staphylococcus aureus* strain; S54F9 *spa*-type t1333 was used for inoculation. This strain has recently been characterized by whole-genome sequencing (12) and used in various porcine models of haematogenous osteomyelitis, endocarditis, encephalitis and sepsis (12). The inoculum of *S. aureus* was prepared as previously described (13) and diluted with sterile 0.9 % isotonic saline in order to obtain inoculation doses/volumes of 10^4, 10^3 or 10^2 CFU in 10 µL.

Blood samples

On the days of surgery and euthanasia, blood samples were taken from the jugular vein. For screening of bacteremia, 2 ml blood samples were collected in heparin tubes and analyzed (13). Additionally, 6-8 ml blood was collected in serum tubes, centrifuged and the recovered serum stored at -80˚C until processing. Stored serum was used for evaluation of the systemic acute phase response by measurement of C-reactive protein (CRP) and serum amyloid A (SAA), respectively by enzyme-linked immunosorbent assay (14, 15).

Macroscopic pathology

Following euthanasia, the surgical wounds were inspected and opened in the first two layers (skin and subcutis). Afterwards, the right hind leg was cut off in the stifle joint. Subsequently, the periosteal sutures were opened and the implant removed from the bone. In 17 pigs (9 sham inoculated Group C animals, 5 Group A animals inoculated with the high dose and 3 Group B animals inoculated with the lower doses) the right tibial bone was sectioned sagittally through the implant cavity in order to allow evaluation of the bone tissue surrounding the implant cavity. The abdomen and thorax of all 30 kg BW pigs were cut open and the organs inspected *in-situ*. In

these animals the major right and left *lnn inguinales profundi* where eviscerated and the length and width registered.

Computer tomographic (CT) scanning

Following euthanasia and removing of the implants, the right hind leg was scanned with a single slide CT scanner (Siemens Somatom Emotion, Erlangen, Germany). Tibia was scanned in the cranio-caudal direction with a slide thickness of 2 mm (kV = 130 and mAs = 55). The scans were reconstructed using a standard soft tissue algorithm (B80s). The following registrations were obtained blinded using the software system Osirix Lite; 1) cortical diameter of the implant cavity, in order to quantify bone destruction around the implant, and 2) CT volumetry of the implant cavity and associated osteomyelitis if present, in order to quantify the total volume of bone destruction (16). Pigs of 67-77 kg BW had 0.25 cm^3 subtracted from their volume of changes, corresponding to the extra length of the implant cavity in these animals.

Microscopic pathology

Following removal of the implants, and sagittal sectioning if performed, all left (non inoculated) and right (inoculated with saline or bacteria) tibial bones were placed in 10 % formalin. Additionally, a sample from the lung, liver, left kidney and spleen were also fixed in formalin. For the osseous tissue, formalin fixation was followed by decalcification (13). Following fixation in formalin or decalcification, all tissues were cut into representative pieces and processed through graded concentrations of alcohol and embedded in paraffin wax. Tissue sections (4–5 µm) were stained with haematoxylin and eosin (HE). On a section from the bone piece containing the center of the implant cavity, the peri-implanted pathological bone area (PIBA) was measured perpendicular to the implant cavity. PIBA was defined as the distance from the

beginning of the implant cavity until normal pattern of trabecular bone and bone marrow appeared. The number of bacterial aggregates were registered inside PIBA and in selected cases immunohistochemical (IHC) staining for *S. aureus* was performed (13). On the same sections, the number of neutrophil granulocytes (NG) inside PIBA were counted by the method developed by Morawietz *et al*. (17). Briefly, first potential hot spots rich in NG were identified at low magnification. These areas were then evaluated under high power (x 400 magnification) and all cells clearly identifiable as NG were counted. In each high power field (HPF), a maximum of 10 NG was counted. Ten HPFs were examined in this way, resulting in a maximum count per pig of 100 NG (17). All PIBA measurements and NG counts were obtained blinded.

Microbiology

Following removal of the implants, a swab was taken from the implant cavity of all Group A and Group B animals and from four Group C animals and analyzed as previously described (18). Selected isolates of bacteria were *spa*-typed (19). The caudal part of the left lung lobe was collected for quantitative microbiology as well (18).

Implants

All implants were removed from the tibial bones with a sterile lancet, or by shaking the leg over a sterile drape. Selected implants (13 implants from Group A pigs and 2 implants from Group B pigs) were placed in 10% formalin for peptide nucleic acid fluorescence *in-situ* hybridization (PNA FISH) (20). A *S. aureus* specific probe (21) was used to visualize if the bacterium had attached to the surface of the implants. The evaluation of implants was blinded.

Statistics

For comparing the size of the regional lymph nodes and PIBA, the NG count and the CT measurements between Group A, B and C, the Kruskal-Wallis test was used followed by multiple comparisons using Dunn's test. A repeated measurement ANOVA, followed by multiple comparisons using Sidak's test, was performed for the acute phase response. Receiver-operating characteristic (ROC) curves were generated to examine the sensitivity and specificity between NG counts and clinical (CT scans) and microbiological (inoculated vs. sham inoculated) diagnoses depending on different thresholds. All calculations were performed using Prism version 7 (Graphpad Software, Inc, California, USA). Statistical significance was assigned to differences having P-values ≤ 0.05.

Results

Insertion of implants

Implants were placed at the intended position, *e.g.* 10 mm below the growth plate in 40 out of 42 cases. In two cases the position was too close to the growth plate, although still placed within trabecular bone tissue. In one case intensive bleeding occurred from the implant cavity immediately after inoculation. This animal (Group A1) was excluded from the study due to an uncertain infectious inoculum dose.

Clinical observations

After recovery from anesthesia, all pigs were lame on the inoculated leg. However, they were able to use the leg and walked freely around in the pens. During the first day the lameness diminished and disappeared 2 to 3 days after inoculation in 39 out of 41 pigs. Due to persistent

lameness and fewer, two pigs received intramuscular injections of 0.1 mg/kg BW of buprenorphine (0.3mg/ml) every 6-8 hour until euthanasia. All animals ate and drank normally throughout the experiment.

Blood samples

Bacteremia was not observed in any of the animals. The medians for CRP and SAA are presented in Figures 2A and 2B. For both acute phase proteins, a significant increase was seen in Group A pigs compared to control animals (CRP; P=0.0002, SAA; P=0.05).

Macroscopic pathology

Wound infections, present as rupture of skin sutures and inflammation of underlying tissue, were observed in 2 out of 10 control animals (Group C) and in 4 out of 31 infected animals (Group A + B). Formation of an abscess in the subcutaneous tissue in connection with the implant cavity was not seen in any of the 10 control animals (Group C), whereas it was present in the 25 animals infected with 10^4 CFU (Group A) and in 2 out of 6 animals infected with 10^2 or 10^3 CFU (Group B). In 17 pigs exposed to sagittal sectioning of the right tibial bone, osteomyelitis was never seen around the implant cavity in the 9 control pigs, whereas, it was present in 5 out of 5 animals injected with 10^4 CFU and 1 out of 3 injected with 10^3 CFU (Figs. 2C + 2D). The osteomyelitis lesion consisted of a demarcated area of sequestrated bone tissue intermingled with pus. Macroscopic lesions were not seen in any of the other organs. The length and width of the largest right and left *lnn inguinales profundi* were added and divided by 2 (Fig. 2E). The difference between the right and left regional lymph node size is shown in Figure 2F. The difference was significantly bigger in both Group A and B animals compared to the control animals of Group C (P = 0.0004 and 0.0024, respectively).

CT scanning

Signs of osteomyelitis was seen in 20 out of 24 Group A animals, and in 1 out of 3 Group B animals, whereas it was absent in the control animals of Group C. In cases with no signs of osteomyelitis, the estimated volume of changes (CT volumentry) represented only the implant cavity (Fig. 3A). The estimated volume of changes was significantly (P = 0.007) higher for Group A animals compared to Group C animals (Figs. 3B + 3C). The cortical diameter of the implant cavity in pigs receiving the high bacterial dose (Group A) increased significantly (P = 0.0151) compared to the control group (Fig. 3D). Furthermore, cortical sequesters were seen in 7 animals from Group A. Significant differences were not observed for any of the parameters measured by CT between Group B and C.

Microscopic pathology

The estimated size of PIBA was significantly (P = 0.0331) higher for Group A animals compared to the control animals of Group C (Fig. 4A). A significance was not seen between Group B animals infected with the lower bacterial doses and control animals. In all control animals belonging to Group C, PIBA consisted of an interrupted thin layer of elongated fibroblasts and inflammatory cells lining compressed and osteonecrotic trabecular bone tissue. This layer was sporadically intermingled with single neutrophils and osteoclasts and surrounded by edema and proliferation of fibroblast and osteoblast blending into the adjacent bone tissue and bone marrow. A different pattern of PIBA was seen in Group A animals infected with the high bacterial dose. In these animals, a cellular layer of fibroblasts, neutrophils, macrophages, giant cells and sometimes debris of necrotic bone tissue were seen bordering the implant cavity. Outside this cellular layer osteonecrosis and osteoclasts were seen. As in the control animals, an outermost

osteogenic and fibroblast layer was also present, although with more fibroplasia. Pigs of Group B (lower doses) showed either the same changes of PIBA as seen in Group A, but not as extensive, or as the control pigs of Group C. No lesions were seen within the left tibial bone, liver, lung, spleen or kidney in any of the animals. In general, bacteria were identified within the exudate of the implant cavity and inside PIBA. In Groups A and B, bacteria were identified in PIBA of 15 out of 25 and 2 out of 6, respectively. Bacteria within PIBA stained positive for *S. aureus* in all samples selected for IHC (Fig. 4D). Bacterial colonies were not identified within PIBA of any of the control animals.

The NG count differed significantly (P = 0.0001) between infected Group A pigs receiving the high bacterial dose and the non infected control animals of Group C (Fig. 4E). Within Group B, receiving the lower bacterial dose, the NG numbers varied widely (Fig 4E). By analyzing the ROC curve (The area under the concentration-time curve (AUC) = 0.94), the threshold for histopathological differentiation between inoculated (Group A) and sham inoculated animals (Group C) was 40 NG in 10 HPFs. This threshold resulted in a sensitivity of 92 % and a specificity of 90 % for diagnosing bacterial infection. Two of 25 Group A pigs had a NG count below 40. When the NG counts were correlated with a positive or negative diagnosis of osteomyelitis based on CT scans (AUC = 0.90), the threshold of 40 NG in 10 HPFs resulted in a sensitivity of 94 % and a specificity of 71.4%. Once again the NG count was significantly (P= 0.0001) higher for pigs diagnosed with osteomyelitis by CT-scanning (Fig. 4F). Group B animals were not included in ROC calculations due to the large variability within this group. A positive correlation was seen between a high NG count and high values of SAA, CRP, regional lymph node size, PIBA size, CT volumetry of lesions and cortical diameter of the implant cavity, see Fig.5.

Microbiology

Swabs from the implant cavity demonstrated *S. aureus* in 23 out of 25 pigs from Group A inoculated with 10^4 CFU. The remaining two pigs showed contamination. In Group B pigs inoculated with 10^2 or 10^3 CFU, *S. aureus* was cultured in 3 animals, enterococci species in 2 animals, and 1 animal was sterile. In the control animals of Group C *S. aureus* was not cultured. All 42 lung samples were sterile. *Spa*-typing of isolates confirmed *S. aureus* strain t1333 (used for inoculation) in all *S. aureus* positive isolates from Groups A and B animals.

Implants

By PNA FISH all implants from Group B were negative for *S. aureus*. Within Group A, inoculated with the high bacterial dose, PNA FISH positive implants were seen in 7 out of the 13 investigated cases.

Discussion

In this paper a novel low-inoculum *S. aureus* porcine model of IAO was presented. The model successfully replicated the pathogenesis of external contamination during insertion of bone implants and prosthesis in humans (1). An objective quantification protocol was used to characterize the model, including estimation of the systemic acute phase response, regional lymph node size, volume of bone lesions and numbers of NGs surrounding the bone implant. The model of IAO inoculated with 10^4 CFU of *S. aureus* showed significant results on all parameters when compared to sham inoculated control animals. No difference was observed between the subgroups of Group A (30 kg BW vs. 67-77 kg BW), Group B (10^2 vs. 10^3 CFU) and Group C (implant vs. no implant).

The present study showed a clear correlation between the number of injected bacteria and development of IAO. Pigs of Group B, inoculated with the lower doses (10^2 or 10^3 CFU), were not significantly different from the control animals of Group C on any of the parameters, except for an increase in the size of local lymph nodes. Therefore, the high dose of 10^4 CFU is considered the lowest useful inoculation dose in further studies using the present porcine model. The high dose was not associated with secondary spread of the bacteria, as no animal developed bacteremia or had embolic lesions in any organs. Previously, only two porcine models of IAO, *e.g.* based on traumatic inoculation of bacteria, have been described. The first porcine model was published in 1970 by Koschmieder *et al.* who created a 1 x 2 cm femoral cortical window and inoculated 2 x 10^8 CFU of *S. aureus* (7). The model was used for testing the effect of gentamicin-impregnated PMMA bone cement. The other model was developed by Patterson *et al.* in 1993 (8). In that study osteomyelitis was induced in the mandible of 8 adult miniature pigs by drilling a hole in the mandible. Afterwards sodium morrhuate (sclerosing agent) and 10^9 CFU of *S. aureus* was injected and either PMMA bone cement or bone wax inserted. Clearly, the optimal dose of 10^4 CFU used for inoculation in the present model is a remarkable reduction in the number of bacteria used compared to the two former porcine models. With the dose of 10^4 CFU it was possible to re-isolate the same bacterial *S. aureus* strain as used for inoculation in all but 2 animals (showing contamination) using cotton swabs. Therefore, it was concluded that the infection occurred due to the inoculated strain. However, cotton swabs are not a recommended tool for making microbiological diagnosis of bone infections in patients (22). In regards to bacterial attachment to the implant surface PNA FISH showed a low sensitivity. In previous studies, PNA FISH has been highly sensitive for identification of bacteria in tissue sections. However, the geometry of the present implants hampered a full examination of the entire surface.

Recently, it was reported that sonication (implants are sonicated in an ultrasonic bath and the fluid from the sonication is cultured) improves the detection of microorganisms attached to an implant (23). Therefore, in future studies using the porcine model whole tissue samples and sonication of implants (23) are recommended to obtain microbiological diagnosis and estimate the number of bacteria attached to the implant surface.

All orthopedic implants will develop a peri-prosthetic membrane between bone tissue and the implant (24). In well-fixed implants these membranes are considerably smaller than 1.0 mm compared to cases of aseptic and septic loosening of bone implants and prosthesis (25). In agreement with this, the control group in the present study showed a thin layer of cells towards the implant cavity and PIBA with values below 1.02 mm. Recently a study demonstrated that bone changes (primarily osteonecrosis) occur up to 1.2 mm around an inserted K-wire without bacterial inoculation (26). This is also comparable to the present study, in which it is believed that some parts of PIBA developed due to drilling of the implant cavity.

In humans, the peri-prosthetic membrane is defined as a fringe of connective tissue (27). The peri-prosthetic membrane can be classified into four different types all of which are associated with clinical disease (27). The histopathological findings of Group A pigs can be categorized under the type II Peri-prosthetic membrane of the infectious type. Type II is further divided into low and high grade of infections (24, 27). Furthermore, the morphology of bone lesions in all Group A animals were compatible with score 2, 3 or 4 in the scoring system developed by Petty et al. representing different levels of increase in polymorph nuclear leucocytes, microabcesses and soft tissue abscesses (28). Histology is considered one of the golden standards for the diagnosis of prosthetic joint infections, and samples from the peri-prosthetic membrane is the best specimen for the histological diagnosis of IAO (29). Therefore, the NG counts of the preset

study was conducted within PIBA, which contained a cellular layer and extracellular components, *e.g.* it is comparable to the peri-prosthetic membrane (27). A threshold of 23 infiltrating NG in 10 high power fields has been recommended for the histopathological diagnosis of septic loosening of prosthesis in humans (17), without taking the grade of infection into account (high or low grade). This threshold had a sensitivity of 73 % and a specificity of 95 % when compared with the microbiological diagnosis (17). In the present study, a threshold of 40 NG in 10 HPF resulted in sensitivity and specificity values within the same range, although with a reduced risk for a false positive outcome as the diagnostic sensitivity was 92 %. Based on the present results, the porcine model of IAO (Group A pigs) represents a high grade infection. Therefore, the present estimate of approximately 40 NG in 10 HPF could be recommended as a cut-off value for histopathological diagnosis of high grade IAO. A cut-off value specific for high grade prosthetic infections in humans has not been defined (27). In the porcine model, high NG counts were associated to the highest measured values on all parameters (Fig. 5). Therefore, the porcine model of IAO showed a reliable logic connection between a high inflammatory response vs. size of bone lesions and regional and systemic responses (Fig. 5).

In humans, clinical signs of IAO are typically seen several months or years following insertion of bone prosthesis (1). This time pattern is difficult to replicate in an animal model. However, animal models with an earlier onset of infection are still reliable, as the histopathological diagnosis of IAO is dependent on finding NGs (30). The most popular animal species for modeling IAO are rodents and rabbits (31). However, pigs are closely related to humans in term of immunology, anatomy and physiology and represent an excellent animal model for studying infectious diseases like IAO (6). In 2016 it was shown, that the porcine and murine immune systems show 80 and 20 percent similarity to humans, respectively (6). Furthermore, similar to

humans, and in contrast to rodents (32), pigs have high numbers of neutrophils in the peripheral circulation (50-70%). In addition to the immunological similarities, porcine bone mineral density, anatomy, morphology, remodeling rate and healing are also similar to humans (33). Of disadvantages in using pigs as models, it should be mentioned, that the bone growth of conventional pigs is very fast. This might, however, be circumvented by using Minipigs. Furthermore, the length of the porcine tibia and femur is relatively short compared to humans, which in some cases might complicate direct testing of human-designed implants. However, compared to rodents and rabbits, the porcine bone size allows sampling of larger quantities for various purposes. Recently, the use of small ruminants for modeling of IAO has increased (34), despite there being several important differences to human bones such as seasonal bone loss (35) and higher trabecular density (36). Furthermore, the ruminant gastrointestinal system, like the pseudoruminant system of rabbits, will affect the results when such models are used for testing antibiotic treatments. In contrast, pigs provide an adaptable model to evaluate the efficacy of oral and systemic antibiotic treatment due to their omnivore physiology.

The porcine model is a useful, reliable and discriminative tool for examining several different aspects of IAO in humans, *e.g.* the impact of different implant surface coatings, vaccination against *S. aureus*, virulence factors, new diagnostic tests and medical and surgical treatment regimes.

Acknowledgement

We thank Betina Andersen and Elizabeth Petersen for their excellent laboratory assistance. This study was financed by grant no. 4005-00035B from the Danish Medical Research Council and the European Union's Horizon 2020 research and innovation programme under NOMORFILM project grant agreement No 634588.

References

1) Kapadia BH, Berg RA, Daley JA, *et. al*. 2016. Periprosthetic joint infections. The Lancet 387: 386-394.
2) Jorgensen PN, Meyer R, Dagnaes-Hansen F, Fuursted K, Petersen E. 2014. A modified chronic infection model for testing treatment of *Staphylococcus aureus* biofilms on implants. PLOS ONE 9: 1-7.
3) Krenek L, Farng E, Zingmond D, *et al*. 2011. Complication and revision rates following total elbow arthroplasty. J Hand Surg Am 2011 36: 68–73.
4) Lee J, Kang C-I, Lee JH, *et al*. 2010. Risk factors for treatment failure in patients with prosthetic joint infections. J Hosp Infec 2010 75: 273-276.
5) Marculescu CE, Berbari EF, Hanssen AD, *et al*. 2006. Outcome of prosthetic joint infections treated with debridement and retention of components. CID 42: 471-478.
6) Meurens F, Summerfield A, Nauwynck H, *et al.* 2012. The pig: a model for human infectious diseases. Trends in Microbiology 20: 50-57.
7) Koschmieder R, Ritzerfeld W, Homeyer L. 1975. Gentamycinzusatz zum polymethylmethacrylat zur behandlung von Knocheninfektionen. Z Orthop 975 113: 147-9.
8) Patterson AL, Galloway RH, Baumgartner JC, Barsoum IS. 1993. Development of chronic mandibular osteomyelitis in a miniswine model. J Oral Maxillofac Surg 51: 1358-62.
9) Harris DL, Alexander TJL. Methods of Disease Control. In: Diseases of Swine. Taylor DJ, Mengeling WL, Dállaire SY, Straw BE, editors. Iowa: Iowa State University Press, 1999.

10) Tøttrup M, Bue M, Koch J, *et al*. 2016. Effects of Implant-associated Osteomyelitis on Cefuroxime Bone Pharmacokinetics - Assessment in a Porcine Model. J Bone J Surg 98:363-369.

11) Johansen LK, Svalastoga EL, Frees D, *et al*. 2013. A new technique for modeling of haematogenous osteomyelitis in pigs: inoculation into femoral artery. J Invest Surg 26: 149-153.

12) Aalbæk B, Jensen LK, Jensen H, *et al.* 2015. Whole Genome Sequence of Staphylococcus aureus S54F9 isolated from a Chronic Disseminated Porcine Lung Abscess and used in Human Infection Models. GenomeAnnounc 3: 1.

13) Johansen LK, Frees D, Aalbaek B, *et al*. 2011. A porcine model of acute, haematogenous, localized osteomyelitis due to *Staphylococcus aureus*: a pathomorphological study. APMIS 119: 111-8.

14) Heegaard PMH, Pedersen HG, Jensen AL, Boas U. A robust quantitative solid phase immunoassay for the acute phase protein C-reactive protein (CRP) based on cytidine 5'-diphosphocholine coupled dendrimers, J. Immunol. Meth. 343, 112-118, 2009.

15) McDonald TL, Weber A, Smith JW. A monoclonal antibody sandwich immunoassay for serum amyloid A (SAA) protein, J. Immunol. Methods (1991) 144:149-155.

16) Van der Vorst JR, Van Dam RM, Van Stiphout RSA, *et. al*. 2010. Virtual liver resection and volumetric analysis of the future liver remnant using open source image processing software. World J Surg 34: 2426-2433.

17) Morawietz L, Tiddens O, Mueller M, *et. al.* 2009. Twenty three neutrophil granulocytes in 10 high power fields is the best histological threshold to differentiate between aseptic and septic endoprosthesis loosening. Histopathology 54: 847-853.

18) Jensen HE, Nielsen OL, Agerholm JS, *et al*. 2010. A non-traumatic *Staphylococcus aureus* osteomyelitis model in pigs. In Vivo 24: 257-64.

19) Stegger M, Andersen PS, Kearns A, *et al.* 2012. Rapid detection, differentiation and typing of methicillin-resistant *Staphylococcus aureus* harbouring either mecA or the new mecA homologue mecA(LGA251). Clin Microbiol Infect 18: 395-400.

20) Jensen LK, Koch J, Aalbæk B, *et. al*. 2016. Early implant associated osteomyelitis results in a peri-implanted bacterial reservoir. APMIS. In Press.

21) Bjarnsholt T, Jensen PO, Fiandaca MJ, Pedersen J, Hansen CK, *et. al*. 2009. *Pseudomonas aeruginosa* biofilms in the respiratory tract of cystic fibrotic patients. Pediatric Pulmonology: 44; 547-558.

22) Aggarwal VK, Higuera C, Deirmengian G, Parvizi J, Matthew AS. 2013. Swab cultures are not as effective as tissue cultures for diagnosis of periprosthetic joint infections. Clin Orthop Relat Res 471: 3196-3203.

23) Song Z, Borgwardt L, Høihy N, Hong W, Sørensen TS, Borgwardt A. 2013. Prosthesis infections after joint replacement: the possible role of bacterial biofilms. Orthop reviews 5: 65-71.

24) Mowarits L, Classen RA, Schroeder JH, *et. al.* 2006. Proposal for a histological consensus classification of the periprosthetic interface membrane. J clin Path 59: 591-597.

25) Bos I. 2001. Tissue reactions around loosened hip joint endoprosthesis. A histological study of secondary capsules and interface membrane. Orthopade 30: 881-889.

26) Franssen BB, Van Diest PJ, Schuurman AH, Kon M. 2007. Drilling K-wires, what about osteocytes? An experimental study in rabbits. Arc orthop traum surg 128: 3174-3183.

27) Krenn V, Morawietz L, Perino G, *et al*. 2014. Revised histopathological consensus classification of joint implant related pathology. Pathol Res Prac 210: 779-786.

28) Petty W, Spanier S, Shuster J, Silverthorn C, Gainesville F. 1985. The Influence of Skeletal Implants on Incidence of Infection. J Bone J surg Am 67: 1236-1344

29) Bori G, Munzo-Mahamud E, Garcia S, *et. al.* 2011. A. Interface membrane is the best sample for histological study diagnose prosthetic joint infection. Mordern Pathology 24: 579-584.

30) Tsaras G, Maduka-Ezeh A, Inwards CY, *et al*. 2012. Utility of intraoperative frozen section Histopathology in the diagnosis of periprosthetic joint infection. J Bone J Surg Am 94: 1700-1711.

31) An YH, Kang QK, Arciola CR. 2006. Animal models of osteomyelitis. Int J Artif Organs 29: 407-20.

32) Fairbairn L, Kapetanovic R, Sester DP, Hume DA, *et al.* 2011. The mononuclear phagocyte system of the pig as a model for understanding human innate immunity and disease. J Leukoc Biol 6: 855–871.

33) Reichert JC. Saifzadeh S, Wullschleger ME *et el.* 2009. The challenge of establishing preclinical models for segmental bone defect research. Biomaterials 30: 2149-2163.

34) Wancket LM. 2015. Animal models for evaluation of bone implants and devices comparative bone structure and common model uses. J Vet Pat 1015: 1-9

35) Bonucci E, Ballanti P. 2014. Osteoporosis – bone remodelling and animal models. Toxicol Pathol 42: 957-696

36) Nafei A, Danielsen CC, Linde F *et. al*. 2000. Properties of growing trabecular ovine bone, part I: mechanical and physical properties. J Bone J Surg Br 82: 910-920.

Table and figure legends

Table 1

Study design of the novel porcine model of implant associated osteomyelitis and overview of allocation of animals into Groups A, B and C. *PI; post inoculation, ** One animal was excluded based on a surgical complication during insertion of bone implant.

Figure 1

The surgical procedure used for insertion of a bone implant in the porcine model of implant associated osteomyelitis. A: Equipment used for insertion of a steel implant of 2 x 15 mm (a) and inoculation of *S. aureus* bacteria (b). B: the implant (the end is seen in the picture (arrow)), was inserted proximally on the medial side of the right tibia. C: The position of the implant (10 mm distal and parallel to the growth plate) was achieved with mobile fluoroscopy during surgery. D: After surgery the periosteum, subcutis, and skin was closed.

Figure 2

Systemic, regional and local reaction to experimentally induced implant associated osteomyelitis in the porcine model. Level of significance: *<0.05, **≤0.01, ***≤0.001. Groups A and B were inoculated with *S. aureus* bacteria and Group C with saline. Median and 95 % confidence interval. A: Serum levels of C-reactive protein. A significant increase was seen in Group A. B: Serum levels of Serum Amyloid A. A significant increase was seen in Group A. C: Tibia from a control pig, signs of osteomyelitis was not present around the implant cavity (ic) five days after inoculation with saline. D: Tibia from an infected pig, signs of osteomyelitis (o) was seen around the implant cavity (ic) five days after inoculation with 10^4 CFU of *S. aureus*. E: left (l) and right

(r) regional lymph node from an animal inoculated with 10^4 CFU of *S. aureus*. Bar = 8 mm F: Scatter dot plot with median of the right and left regional lymph node sizes (length and wide divided by 2). The right lymph nodes were significantly enlarged for both Group A and Group B when compared to Group C.

Figure 3

Computer tomographic (CT) scans of the right tibia in the porcine model of implant associated osteomyelitis. Level of significance: *<0.05, **≤0.01, ***≤0.001, ****≤0.0001. A and B: The green lines surround the area used for volumetry and the yellow lines show how the cortical diameters were measured. A: Tibia from a control pig, signs of osteomyelitis was not present around the implant cavity (ic) five days after inoculation with saline. B: Tibia from an infected pig, signs of osteomyelitis (o) was seen around the implant cavity (ic) five days after inoculation with 10^4 CFU of *S. aureus*. C: Scatter dot plot with median of the volume of implant cavity plus volume of osteomyelitis lesions if present are depicted. The volume was significantly larger for pigs inoculated with 10^4 CFU of *S. aureus* compared to pigs inoculated with saline. D: Scatter dot plot with median of the cortical diameter of the implant cavity are shown. The diameter was significantly larger for pigs inoculated with 10^4 CFU of *S. aureus* compared to pigs inoculated with saline.

Figure 4

Histopathological results in the porcine model of implant associated osteomyelitis euthanized five days after inoculation. Level of significance: *<0.05, **≤0.01, ***≤0.001, ****≤0.0001. A: Scatter dot plot with median of the peri-implanted pathological bone area (PIBA). Groups A and B were inoculated with *S. aureus* bacteria and Group C with saline. The size of PIBA was

significantly larger for pigs inoculated with 10^4 CFU of *S. aureus* compared to pigs inoculated with saline. B: Implant cavity (ic) and surrounding bone pathology of a pig inoculated with saline. Necrotic trabecular bone fragments (n) were seen adjacent to the implant cavity. HE, Bar = 100 μm. C: Implant cavity (ic) and surrounding bone pathology of a pig inoculated with 10^4 CFU of *S. aureus*. Necrotic bone tissue (n) and accumulation of neutrophil granulocytes (ng), giant cells (arrow), macrophages and fibroblasts were present next to the implant cavity. HE, Bar = 100 μm. D: PIBA of a pig inoculated with 10^4 CFU of *S. aureus*. A colony of positive *S. aureus* bacteria (red) are surrounded by neutrophil granulocytes (ng). IHC, Bar = 50 μm. E: Scatter dot plot with median of the distribution of neutrophil granulocytes (NG) in PIBA of animals inoculated with a high dose, lower doses or sham inoculated. The NG number was significantly higher in pigs inoculated with 10^4 CFU of *S. aureus* compared to pigs inoculated with saline. F: Scatter dot plot with median of the distribution of NG in comparison with the results of the CT scans (osteomyelitis: red, no osteomyelitis: green). The NG number was significantly higher in pigs CT-diagnosed with osteomyelitis.

Figure 5

Association between numbers of neutrophils (NG) around the bone implant and serum SAA concentrations, serum CRP concentrations, difference in regional lymph node size, size of peri-implanted pathological bone area (PIBA), cortical diameter of implant cavity, and volume of bone lesion in the porcine model of implant associated osteomyelitis (IAO). Pigs inoculated with 10^4 CFU of *S. aureus* (red) or saline (green) were included.

Table 1

Group	Subgroup	Implant (Steel)	Inoculum	Dose (CFU)	Body weight (kg)	Number of animals	Time of euthanasia PI*
A High dose	A1	2 x 15 mm	*S.aureus*	10^4	30	8**	5
	A2	2 x 20 mm	*S.aureus*	10^4	67-77	18	5
B Lower doses	B1	2 x 15 mm	*S.aureus*	10^3	30	3	5
	B2	2 x 15 mm	*S.aureus*	10^2	30	3	5
C Control	C1	2 x 15 mm	Saline	0	30	7	5
	C2	-	Saline	0	30	3	5

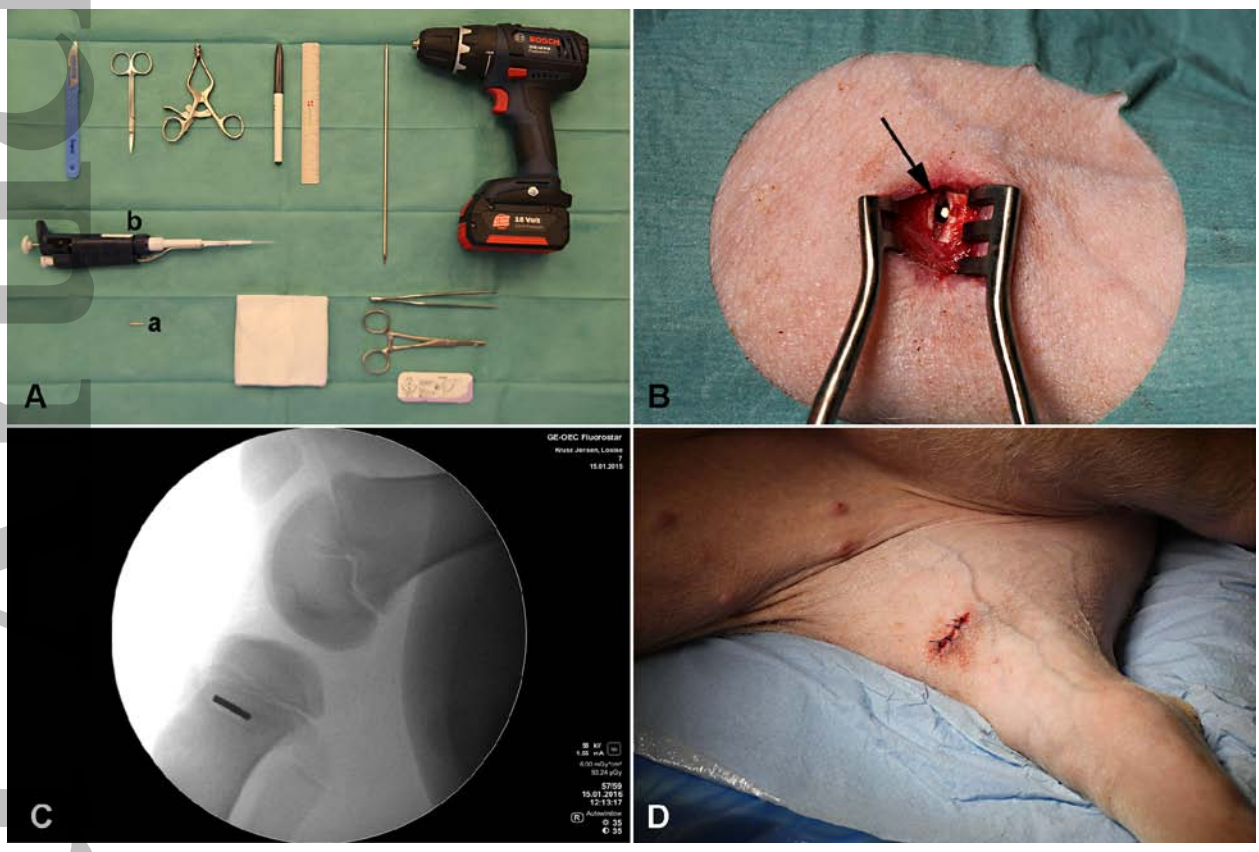

Figure 1

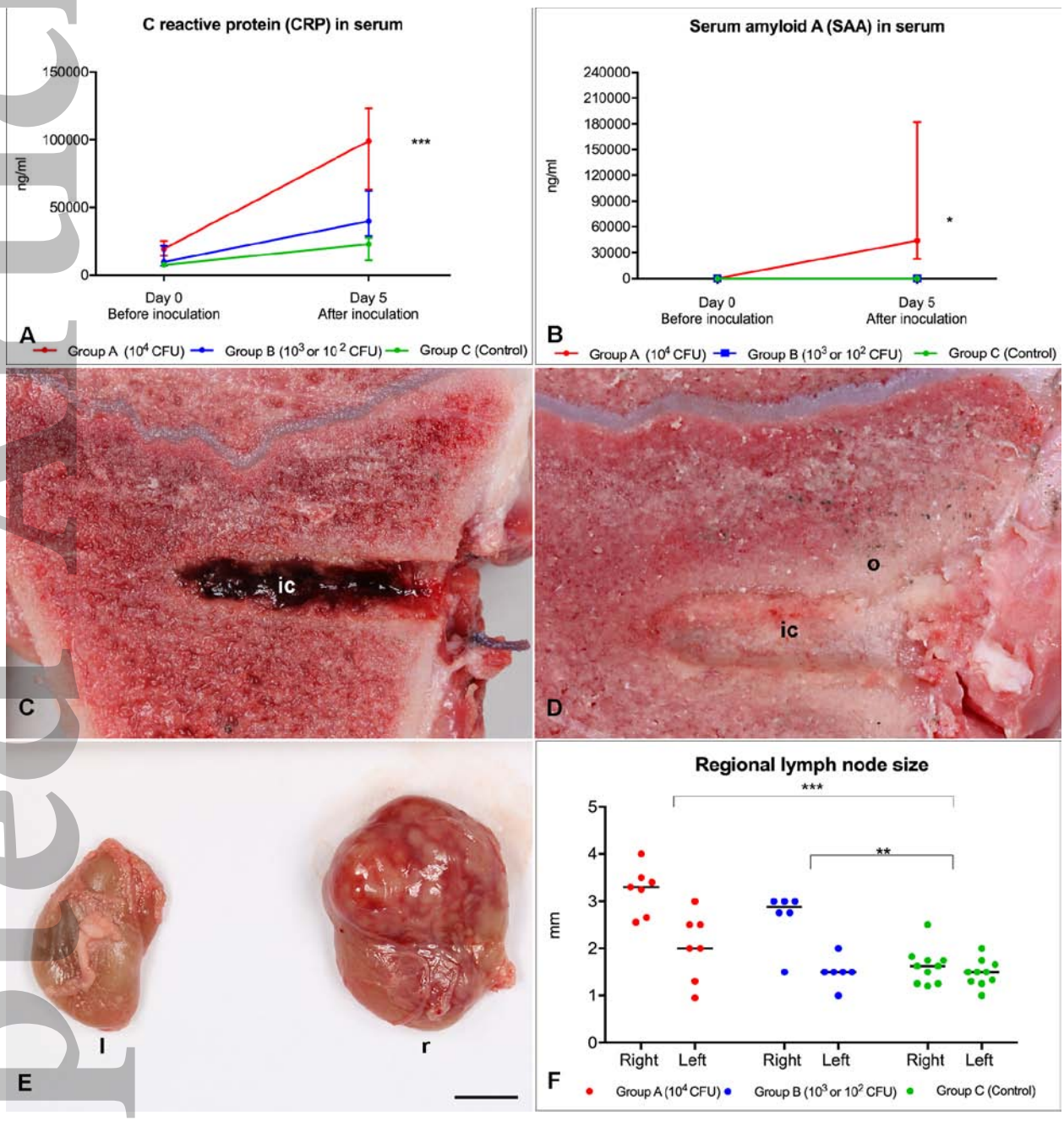

Figure 2

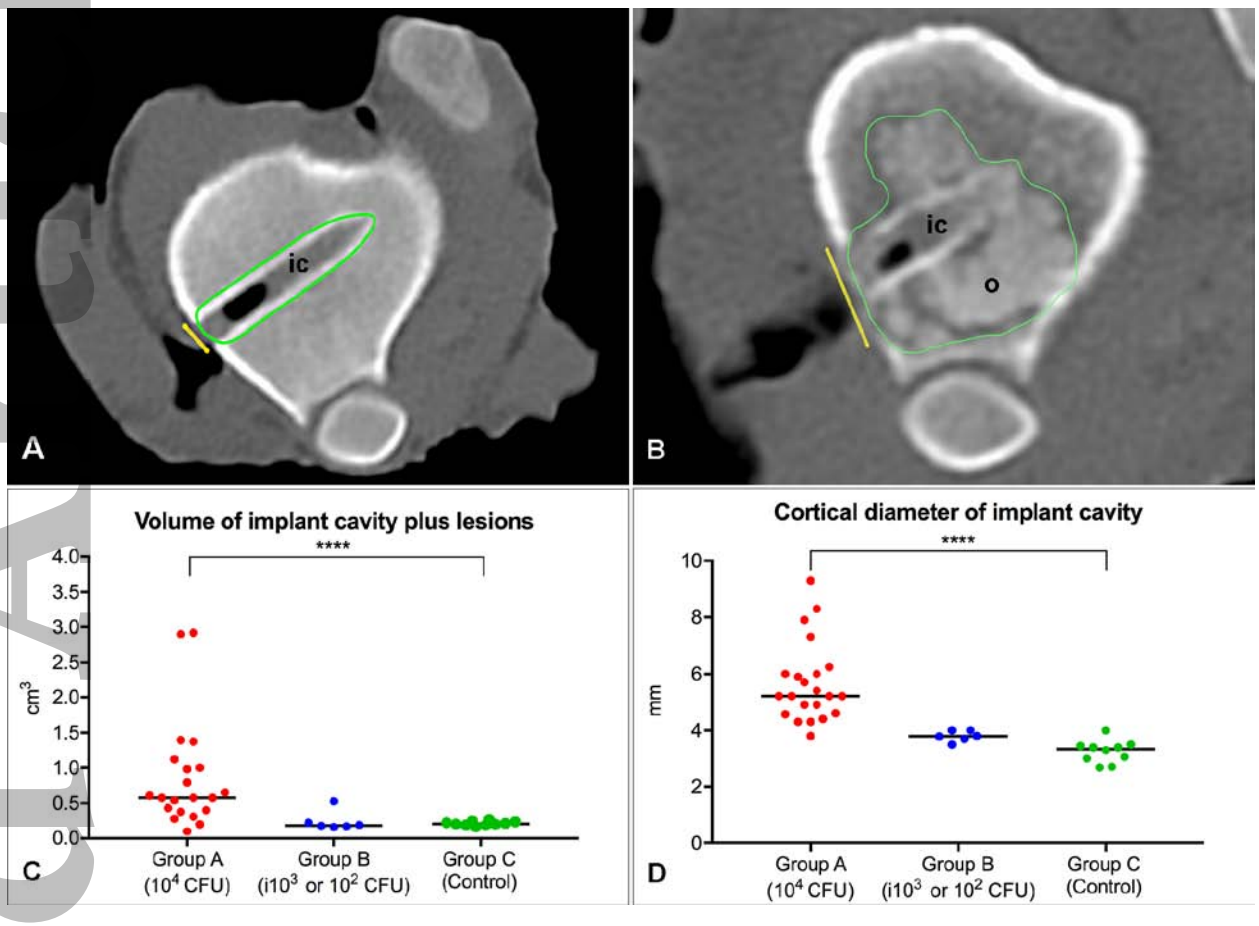

Figure 3

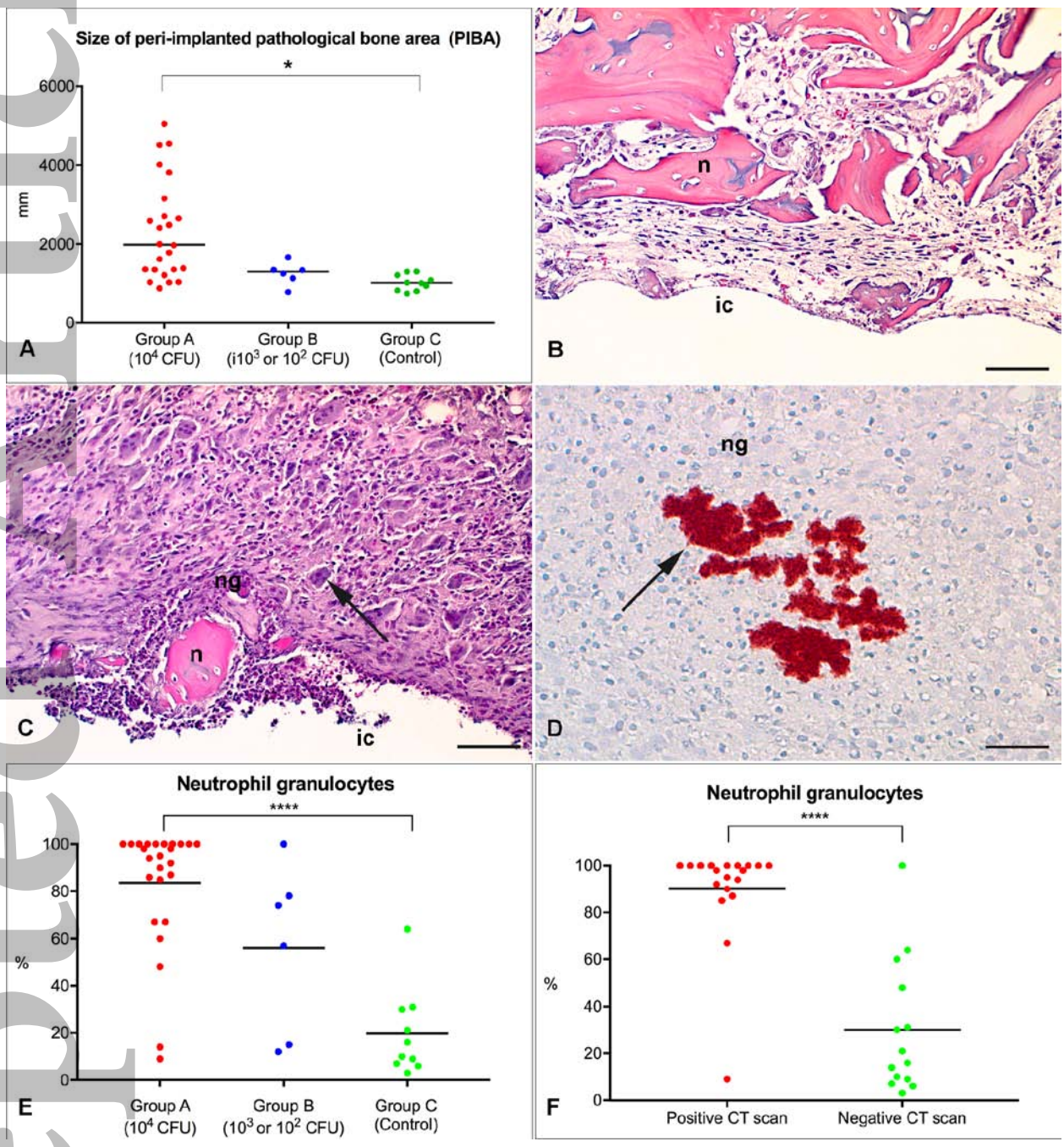

Figure 4

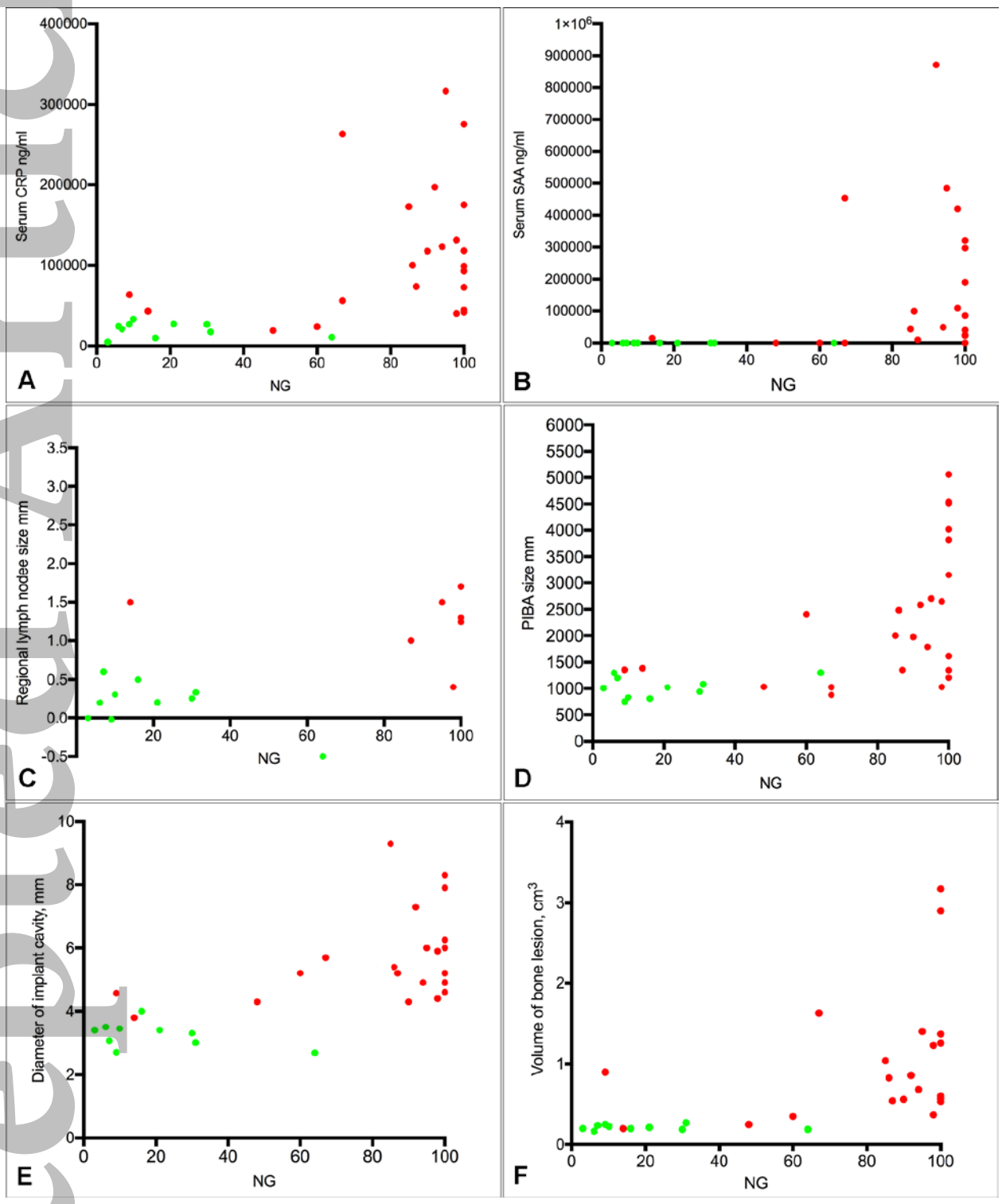

Figure 5